Title: Follow-Up of Lesions with Equivocal Radiotracer Uptake on PSMA-Targeted PET in Patients with Prostate Cancer: Predictive Values of the PSMA-RADS-3A and PSMA-RADS-3B Categories

Running title: PSMA-RADS-3A and PSMA-RADS-3B

Authors: Yafu Yin[1,2], Rudolf A. Werner[1,3], Takahiro Higuchi[3], Constantin Lapa[3], Kenneth J. Pienta[4], Martin G. Pomper[1,4], Michael A. Gorin[1,4], Steven P. Rowe[1,4]

[1]The Russell H. Morgan Department of Radiology and Radiological Science, Johns Hopkins University School of Medicine, Baltimore, MD, USA
[2]Department of Nuclear Medicine, The First Hospital of China Medical University, Shenyang, China
[3]Department of Nuclear Medicine, University Hospital Wuerzburg, Wuerzburg, Germany
[4]The James Buchanan Brady Urological Institute and Department of Urology, Johns Hopkins University School of Medicine, Baltimore, MD, USA

Correspondence:
Steven P. Rowe, MD PhD
Division of Nuclear Medicine and Molecular Imaging
The Russell H. Morgan Department of Radiology and Radiological Science
Johns Hopkins University School of Medicine
601 N. Caroline St. Rm 3233
Baltimore, MD 21287
Tel: +1(734)717-9090
srowe8@jhmi.edu

First author:
Yafu Yin, MD
Division of Nuclear Medicine and Molecular Imaging
The Russell H. Morgan Department of Radiology and Radiological Science
Johns Hopkins University School of Medicine
and
Department of Nuclear Medicine, The First Hospital of China Medical University, Shenyang, China

Word Count:

Figures: 2

Tables: 2

ABSTRACT

Purpose: Prostate-specific membrane antigen (PSMA)-targeted positron emission tomography (PET) imaging has become commonly utilized in patients with prostate cancer (PCa). The PSMA reporting and data system version 1.0 (PSMA-RADS version 1.0) categorizes lesions on the basis of the likelihood of PCa involvement, with PSMA-RADS-3A (soft tissue) and PSMA-RADS-3B (bone) lesions being indeterminate for the presence of disease. We retrospectively reviewed the imaging follow-up of such lesions to determine the rate at which they underwent changes suggestive of underlying PCa.

Methods: PET/CT imaging with ^{18}F-DCFPyL was carried out in 110 patients with PCa and lesions were categorized according to PSMA-RADS Version 1.0. 56/110 (50.9%) patients were determined to have indeterminate PSMA-RADS-3A or PSMA-RADS-3B lesions and 22/56 (39.3%) patients had adequate follow-up to be included in the analysis. The maximum standardized uptake values (SUV_{max}) of the lesions were obtained and the ratios of SUV_{max} of the lesions to SUV_{mean} of blood pool ($SUV_{max\text{-}lesion}/SUV_{mean\text{-}bloodpool}$) were calculated. Pre-determined criteria were used to evaluate the PSMA-RADS-3A and PSMA-RADS-3B lesions on follow-up imaging to determine if they demonstrated evidence of underlying malignancy.

Results: A total of 46 lesions in 22 patients were considered indeterminate for PCa (i.e. PSMA-RADS-3A (32 lesions) or PSMA-RADS-3B (14 lesions)) and were evaluable on follow-up imaging. 27/46 (58.7%) lesions demonstrated changes on follow-up imaging consistent with the presence of underlying PCa at baseline. These lesions included 24/32 (75.0%) PSMA-RADS-3A lesions and 3/14 (21.4%) lesions categorized as PSMA-RADS-3B. The ranges of SUV_{max} and $SUV_{max\text{-}lesion}/SUV_{mean\text{-}bloodpool}$ overlapped between

those lesions demonstrating changes consistent with malignancy on follow-up imaging and those lesions that remained unchanged on follow-up.

Conclusion: PSMA-RADS-3A and PSMA-RADS-3B lesions are truly indeterminate in that proportions of findings in both categories demonstrate evidence of malignancy on follow-up imaging. Overall, PSMA-RADS-3A lesions are more likely than PSMA-RADS-3B lesions to represent sites of PCa and this information should be taken into when guiding patient therapy.

Key words: prostate cancer; prostate-specific membrane antigen; PSMA-targeted PET; PSMA-RADS-3A; PSMA-RADS-3B

INTRODUCTION

In 2018, prostate cancer (PCa) is estimated to be the most commonly diagnosed non-cutaneous malignancy as well as the second most common cause of cancer death in United States men (*1*). Despite how common PCa is, imaging of this malignancy has long been challenging, particularly in patients with recurrent or metastatic disease (*2*). Although conventional imaging can often appropriately stage patients with very advanced disease, it has taken the advent of very sensitive molecular imaging agents to be able to reliably identify small volume disease that may be oligorecurrent/oligometastatic (*3*). Such disease may be amenable to metastasis-directed therapy such as salvage lymphadenectomy or stereotactic body radiation therapy (SBRT) (*4,5*). Those interventions may allow a subset of patients to avoid systemic therapy, and in some cases patients may have prolonged progression-free survival (*6*).

Among the molecular imaging agents for PCa, positron emission tomography (PET)-based radiotracers that target prostate-specific membrane antigen (PSMA) have shown both exceptional sensitivity and specificity (*7,8*). While the improved sensitivity of PSMA-targeted agents relative to conventional imaging has been well-established (*2,7,9*), that superior sensitivity appears to be true even when comparing PSMA-targeted agents to older classes of PCa radiotracers (*10,11*). This has led to the extensive study of PSMA-targeted compounds in PCa biochemical recurrence (*12,13*), partially in the hope that detecting sites of recurrent PCa at low serum prostate specific antigen (PSA) levels may provide new options for metastasis-directed therapy for carefully selected patients. Indeed, as the number of publications on PSMA-targeted

PET has increased, there has been a parallel increase in the number of papers on therapeutic options for oligometastatic PCa (*3*).

With the implication that findings on PSMA-targeted PET will be used to guide therapy, having a standardized framework that demarcates individual lesions and incorporates information about the imaging specialist's confidence that a lesion represents PCa is valuable. One such system that has been proposed is the PSMA reporting and data system version 1.0 (PSMA-RADS version 1.0) (*14,15*). PSMA-RADS is predicated on a 5-point scale with PSMA-RADS-3 indicating an indeterminate lesion. PSMA-RADS-3 can indicate findings, with or without radiotracer uptake, that are unlikely to represent PCa (PSMA-RADS-3C and PSMA-RADS-3D, respectively) (*16,17*). However, in most cases, indeterminate lesions are those findings that would be typical for PCa such as lymph node (PSMA-RADS-3A) or bone lesions (PSMA-RADS-3B) and that have low levels of uptake and lack a correlative anatomic finding. In this study, we have longitudinally followed a series of PSMA-RADS-3A and PSMA-RADS-3B lesions to determine how frequently such findings definitively manifest as sites of cancer involvement.

MATERIALS AND METHODS

Patient Population

110 consecutive patients with a history of pathologically diagnosed PCa who had undergone an ^{18}F-DCFPyL PET/CT scan on a prospective research protocol (ClinicalTrials.gov NCT02825875) were included in this study. Patients were imaged under the auspices of a United States Food and Drug Administration Investigational

New Drug Application (IND 121064). This study was approved by our hospital's Institutional Review Board. All patients signed written, informed consent. Clinical and demographic information including ages, prostate-specific antigen levels, and PCa treatment history were collected.

PET/CT imaging

The radiosynthesis of ^{18}F-DCFPyL was carried out as has been previously described (*18*). Images were acquired in a manner consistent with the methods described by Rowe and colleagues (*19*). In brief, all patients were asked to refrain from eating or drinking for at least 4 hours prior to the intravenous injection of approximately 333 MBq (9 mCi) of ^{18}F-DCFPyL. One hour following the injection, a whole-body PET/CT acquisition was performed (from the mid-thighs through the vertex of the skull) on either a 128-slice Biograph mCT scanner (Siemens, Erlangen, Germany) or a 64-slice Discovery RX scanner (General Electric, Waukesha, Wisconsin, USA). For the acquisitions, the scanners were in 3D emission mode with attenuation correction provided by CT.

Image Analysis

^{18}F-DCFPyL PET/CT scans were centrally reviewed by two experienced readers (YY and SPR) and lesions were categorized according to PSMA-RADS Version 1.0 (*14*). The reviewers reached a consensus on all lesions included in the analysis. As had previously been set forth in the original PSMA-RADS manuscript (*14*), the central reviewers considered PSMA-RADS-3A lesions to be those lymph nodes or soft tissue

findings that were in a typical pattern of distribution for PCa (e.g. pelvis and retroperitoneum, as well as mediastinum and left supraclavicular space in patients with more advanced disease (*20*)). PSMA-RADS-3B lesions could generally be described as sites of low level uptake in the bone without an appreciable anatomic correlate or with punctate sclerosis or other findings on corresponding CT that did not definitively suggest the presence of metastatic disease.

For the patients with lesions categorized with PSMA-RADS-3A and/or PSMA-RADS-3B, longitudinal follow-up imaging data were sought. Patients were included in further analysis if follow-up imaging at least three months after the baseline ^{18}F-DCFPyL PET/CT was available in our institution's Picture Archiving and Communications System. No specific limitations were set on the type of follow-up imaging that could be utilized, and imaging included repeat ^{18}F-DCFPyL PET/CT, diagnostic CT, and/or magnetic resonance imaging (MRI) for evaluation of PSMA-RADS-3A lesions and ^{18}F-DCFPyL PET/CT, diagnostic CT, and/or ^{99m}Tc-methylene diphosphonate (MDP) whole-body bone scan for evaluation of PSMA-RADS-3B lesions.

In addition to PSMA-RADS Version 1.0 categorization, the maximum standardized uptake values (SUV_{max}) corrected for lean body mass for all of the lesions and the mean SUV (SUV_{mean}) of blood pool (determined by a 3-cm sphere in the ascending aorta) were measured. The ratios of SUV_{max} of each lesion corrected for the SUV_{mean} of blood pool ($SUV_{max\text{-}lesion}/SUV_{mean\text{-}bloodpool}$) were calculated.

In regards to the longitudinal follow-up of the PSMA-RADS-3A and PSMA-RADS-3B lesions, central review was again carried out and a consensus was reached as to the nature of the imaging findings on the follow-up studies. Lesions that were

determined on follow-up to be suggestive of the presence of PCa met at least one of the following criteria:

① Follow-up PET/CT imaging with ^{18}F-DCFPyL showed uptake of the radiotracer decreased or increased significantly, determined as an SUV_{max} change of more than 30% after therapy (in analogy to the PERCIST criteria (*21*)) *OR* uptake of the radiotracer increased significantly during observation. This criterion was applied to both PSMA-RADS-3A and PSMA-RADS-3B lesions.

② For PSMA-RADS-3A lesions, follow-up CT or MRI showed the diameters of the lesions either decreased or increased more than 2 mm after therapy *OR* the diameters of the lesions increased more than 2 mm during observation.

③ For PSMA-RADS-3B lesions, the follow-up CT showed new sclerotic or osteolytic changes *OR* baseline faint, indeterminate sclerotic changes demonstrated increased sclerosis.

④ For PSMA-RADS-3B lesions, the follow-up ^{99m}Tc-MDP whole body bone scan showed new avid uptake of radiotracer in the lesions.

Statistical analysis

Fisher's exact test was used to compare the number of PSMA-RADS-3A and PSMA-RADS-3B lesions in different patient groups that were subsequently determined to be true positive for the presence of malignancy. Descriptive statistics were used to evaluate SUV_{max} and $SUV_{max\text{-}lesion}/SUV_{mean\text{-}bloodpool}$ in different types of lesions. $P < 0.05$ was considered statistically significant for any analysis.

RESULTS

Patients

Among the 110 patients, 56 patients (50.9%) were categorized as having at least one PSMA-RADS-3A and/or PSMA-RADS-3B lesion on ^{18}F-DCFPyL PET/CT. However, 34/56 (60.7%) lacked adequate imaging follow-up to definitively assess their lesions in a longitudinal manner. This relatively high rate of patients without adequate follow-up imaging may have been related to multiple factors including patients undergoing metastasis-directed therapy if their ^{18}F-DCFPyL PET/CT scans showed limited sites of disease and achieving complete biochemical responses or seeking second opinions or transferring care after the results of the scans.

The 22/56 (39.3%) remaining patients were included in the subsequent analysis. In regards to available follow-up imaging, 20/22 (90.9%) patients had diagnostic chest/abdomen/pelvis CT scans, 14/22 (63.6%) had whole body BS, 3/22 (13.6%) had abdomen and/or pelvis MRI, and 7/22 (31.8%) had ^{18}F-DCFPyL PET/CT scans. Median follow-up time was 10 months (range 3 – 22 months). Selected demographic and clinical information on these patients is included in Table 1.

Image Analysis

Among the 22 patients with usable longitudinal follow-up, there were a total of 46 lesions designated as PSMA-RADS-3A or PSMA-RADS-3B. 32/46 (69.6%) were categorized as PSMA-RADS-3A, which included 15 retroperitoneal lymph nodes (LNs) (15/32, 46.9%), 13 pelvic LNs (13/32, 40.6%), and four supraclavicular LNs (4/32, 12.5%). All included PSMA-RADS-3A LNs measured much less than 1 cm in axial short

axis diameter (median 0.3 cm, standard deviation 0.1 cm, range 0.2 – 0.5 cm). The uptake characteristics of these lesions are summarized in Table 2.

The remaining 14/46 (30.4%) lesions were categorized as PSMA-RADS-3B. Of these, 12/14 (85.7%) were rib lesions, one was a scapula lesion (1/14, 7.1%), and one (1/14, 7.1%) was an iliac bone lesion. The scapula lesion and two of the rib lesions were occult on conventional imaging with no anatomic correlates. The iliac bone lesion and 10/12 (83.3%) rib lesions demonstrated at least some measure of sclerosis, however the morphology (either faintly visible or punctate) was determined by the central reviewers to not be definitive for metastatic PCa.

In total, 27/46 (58.7%) PSMA-RADS-3A and PSMA-RADS-3B lesions demonstrated changes on follow-up imaging suggesting that they were true positive for PCa involvement (Table 2). Among those 27 lesions, 13/27 (48.1%) met criteria ① and ② from the materials and methods section, 9/27 (33.3%) met criterion ②, 2/27 (7.4%) met criterion ①, 1/27 (3.7%) met criteria ① and ③, 1/27 (3.7%) met criterion ③, and 1/27 (3.7%) met criteria ③ and ④.

In regards to PSMA-RADS-3A lesions, 24/32 (75.0%) demonstrated changes on follow-up imaging consistent with baseline disease involvement (Figure 1). In contradistinction, for PSMA-RADS-3B lesions, 3/14 (21.4%) lesions had findings on follow-up imaging appearing to confirm baseline disease involvement (Figure 2). On a patient level analysis, 15/22 patients (68.2%) had at least one PSMA-RADS-3A or PSMA-RADS-3B lesion undergo changes on follow-up imaging consistent with malignant involvement. In terms of number of lesions per patient, 13/22 (59.1%) patients had a single PSMA-RADS-3A or PSMA-RADS-3B lesion and 9/22 (40.9%)

patients had two or more such lesions (maximum seven). 9/13 (69.2%) solitary lesions had findings on follow-up imaging consistent with disease involvement. For the patients with more than one PSMA-RADS-3A or PSMA-RADS-3B finding, 18/33 (54.5%) lesions in 6/9 (66.7%) patients demonstrated evidence of malignancy on follow-up imaging.

Stratifying by the number of PSMA-RADS-4 and PSMA-RADS-5 lesions present in the same patient on baseline ^{18}F-DCFPyL PET/CT indicated that PSMA-RADS-3A and PSMA-RADS-3B findings were more likely to evidence signs of malignancy on follow-up imaging if other definitively malignant lesions were present. The lesions were divided into three groups: group 1 (n=10) without PSMA-RADS-4 or PSMA-RADS-5 lesions in the same patient, group 2 (n=16) with one to three PSMA-RADS-4 or PSMA-RADS-5 lesions in the same patient, and group 3 (n=20) with more than 3 PSMA-RADS-4 and PSMA-RADS-5 lesions in the same patient. The number of lesions demonstrating evidence of malignancy on follow-up imaging was 3/10 (30.0%) in group 1, 6/16 (37.5%) in group 2 and 18/20 (90.0%) in group 3. The differences among the three groups reached statistical significance ($P < 0.05$).

The SUV_{max}s of PSMA-RADS-3A and PSMA-RADS-3B lesions were similar with overlapping ranges, although the median SUV_{max} of PSMA-RADS-3A lesions was higher than the corresponding median SUV_{max} of PSMA-RADS-3B lesions (median SUV_{max} of PSMA-RADS-3A lesions was 1.62 with a range from 0.93 to 2.32, while the median SUV_{max} of PSMA-RADS-3B lesions was 1.15 with a range from 0.85 to 1.89, respectively) (Table 2). In comparing those lesions that had characteristic changes of malignancy on follow-up imaging versus those that remained unchanged, the median SUV_{max} was actually marginally higher for the unchanged lesions, although again the

SUV_{max} ranges overlapped (median SUV_{max} for changed lesions was 1.53 with a range from 1.05 to 2.32, while the median SUV_{max} for unchanged lesions was 1.30 with a range from 0.85 to 2.09, respectively) (Table 2). Additional characteristics of the lesions can be found in Table 2.

The analyses based on $SUV_{max\text{-}lesion}/SUV_{mean\text{-}bloodpool}$ produced similar results, suggesting that the SUV_{max} ranges encountered for PSMA-RADS-3A and PSMA-RADS-3B lesions are not significantly impacted by blood pool radiotracer concentration at the time of imaging. Median $SUV_{max\text{-}lesion}/SUV_{mean\text{-}bloodpool}$ for PSMA-RADS-3A lesions was 1.64 with a range from 0.90 to 2.81 and for PSMA-RADS-3B lesions the median was 1.18 with a range from 0.77 to 1.63. Again, the ranges of $SUV_{max\text{-}lesion}/SUV_{mean\text{-}bloodpool}$ for lesions with changes suggesting malignancy versus unchanged lesions overlapped (median $SUV_{max\text{-}lesion}/SUV_{mean\text{-}bloodpool}$ for changed PSMA-RADS-3A lesions was 1.65 (range 0.90 to 2.81), median $SUV_{max\text{-}lesion}/SUV_{mean\text{-}bloodpool}$ for unchanged PSMA-RADS-3A lesions was 1.57 (range 1.18 to 1.76), median $SUV_{max\text{-}lesion}/SUV_{mean\text{-}bloodpool}$ for changed PSMA-RADS-3B lesions was 1.23 (range 1.04 to 1.42) and median $SUV_{max\text{-}lesion}/SUV_{mean\text{-}bloodpool}$ for unchanged PSMA-RADS-3B lesions was 1.16 (range 0.77 to 1.63)).

DISCUSSION

PSMA-targeted PET has been rapidly adopted around the world for PCa imaging given its high sensitivity and specificity for the identification of sites of disease (*8*). However, as with any imaging modality, there are indeterminate findings that arise either as a result of incidental findings or because of lesion imaging characteristics that belie

easy categorization (*16*). As a result, multiple systems have been proposed to add structure to the interpretation of PSMA-targeted PET scans (*14,22,23*). While these systems emphasize different aspects of PSMA-targeted PET scan interpretation, the central aspect of PSMA-RADS version 1.0 is the categorization of lesions based on the interpreting imaging specialist's suspicion of the presence of PCa (*14,15*). This aligns PSMA-RADS with previously reported organ-based reporting and data systems such as those for breast (breast imaging reporting and data system, BI-RADS (*24*)) and multi-parametric prostate MRI (prostate imaging reporting and data system, PI-RADS (*25*)). For example, BI-RADS includes a total of seven categories that overall represent different probabilities of imaging findings being malignant and proffer corresponding recommendations (e.g. BI-RADS 3 indicates the need for 6-month follow-up imaging in the context of a less than 2% chance of the finding being malignant, whereas BI-RADS 4 lesions will be found to be cancer at a rate of approximately 30% and BI-RADS 5 lesions are almost certainly cancer with a positive predictive value of about 97% (*24*)). Knowledge of the BI-RADS categories is useful for both radiologists and clinicians for communication and guidance of patient management (*26*).

The potential adoption of PSMA-RADS is contingent upon a similar utility for guiding clinical decision-making. On a global level, nearly 60% of indeterminate lesions on PSMA-targeted ^{18}F-DCFPyL PET/CT were found to have changes on follow-up imaging compatible with disease involvement, with 75.0% of PSMA-RADS-3A lymph node lesions and 21.4% of PSMA-RADS-3B bone lesions meeting our pre-specified criteria for harboring PCa. The presence of more definitive sites of PCa (i.e. PSMA-RADS-4 and PSMA-RADS-5 lesions) increased the likelihood of PSMA-RADS-3A and

PSMA-RADS-3B findings having follow-up imaging findings consistent with the presence of PCa.

These findings bear out that PSMA-RADS-3A and PSMA-RADS-3B are truly indeterminate lesions. Thus, depending on the clinical context, image-guided biopsy or follow-up imaging are required to determine the likelihood of malignancy. In particular, follow-up imaging may be of particular value in isolated PSMA-RADS-3A lesions when there are no other findings on the scan. PSMA-RADS-3B lesions warrant careful consideration as only a minority of such findings will have characteristic changes of PCa involvement on follow-up imaging. If patients are considered for salvage or focal therapies as opposed to systemic therapy, it will be necessary for clinicians to weigh the potential cost and toxicities associated with those therapies against the likelihood of PSMA-RADS-3A and PSMA-RADS-3B lesions representing true sites of disease.

The most significant limitations to the current study are its retrospective nature and that lesions were not correlated to histopathology. As would be expected for indeterminate lesions on PSMA-targeted PET imaging, the findings were often small and would be difficult to reliably target with conventional imaging guidance for biopsy. Therefore, histopathology is a difficult gold standard to apply to this study and follow-up imaging findings may represent a more practical approach to determining the nature of lesions (*2*). Further, because of the small size and/or lack of conspicuity of many PSMA-RADS-3A and PSMA-RADS-3B lesions on conventional imaging, we were unable to apply commonly used response/progression criteria such as RECIST 1.1 (*27*) to objectively categorize findings on follow-up. We also acknowledge that with the often indolent nature of PCa, some lesions which remained unchanged on follow-up imaging

could still represent sites of PCa and that our percentages of PSMA-RADS-3A and PSMA-RADS-3B lesions that we considered consistent with PCa involvement may be underestimated. Prospective longitudinal follow-up of a larger number of indeterminate lesions from PSMA-targeted PET scans will be critical to address these limitations.

CONCLUSION

In this study of longitudinal follow-up of lesions with indeterminate levels of uptake on PSMA-targeted PET, a significant majority (75.0%) of PSMA-RADS-3A lesions demonstrated changes on subsequent imaging compatible with the presence of PCa. However, only a minority (21.4%) of PSMA-RADS-3B indeterminate bone lesions showed changes on follow-up imaging suggestive of underlying PCa. These findings confirm the necessity for a category in the PSMA-RADS grading system for indeterminate lesions.

DISCLOSURE

MGP is a co-inventor on a United States patent covering ^{18}F-DCFPyL and as such is entitled to a portion of any licensing fees and royalties generated by this technology. This arrangement has been reviewed and approved by the Johns Hopkins University in accordance with its conflict of interest policies. MAG has served as a consultant for Progenics Pharmaceuticals, Inc., the licensee of ^{18}F-DCFPyL. All authors have received research funding from Progenics Pharmaceuticals, Inc.

ACKNOWLEDGEMENTS

We gratefully acknowledge funding from Progenics Pharmaceuticals, Inc., the Prostate Cancer Foundation Young Investigator Award, and National Institutes of Health grants CA134675, CA184228, EB024495, and CA183031. This project has received funding from the European Union's Horizon 2020 research and innovation programme under the Marie Sklodowska-Curie grant agreement No 701983.

References

1. Siegel RL, Miller KD, Jemal A. Cancer statistics, 2018. *CA Cancer J Clin.* 2018;68:7-30.

2. Rowe SP, Macura KJ, Ciarallo A, et al. Comparison of Prostate-Specific Membrane Antigen-Based 18F-DCFBC PET/CT to Conventional Imaging Modalities for Detection of Hormone-Naive and Castration-Resistant Metastatic Prostate Cancer. *J Nucl Med.* 2016;57:46-53.

3. Murphy DG, Sweeney CJ, Tombal B. "Gotta Catch 'em All", or Do We? Pokemet Approach to Metastatic Prostate Cancer. *Eur Urol.* 2017;72:1-3.

4. Siriwardana A, Thompson J, van Leeuwen PJ, et al. Initial multicentre experience of (68) gallium-PSMA PET/CT guided robot-assisted salvage lymphadenectomy: acceptable safety profile but oncological benefit appears limited. *BJU Int.* 2017;120:673-681.

5. Henkenberens C, von Klot CA, Ross TL, et al. (68)Ga-PSMA ligand PET/CT-based radiotherapy in locally recurrent and recurrent oligometastatic prostate cancer : Early efficacy after primary therapy. *Strahlenther Onkol.* 2016;192:431-439.

6. Tosoian JJ, Gorin MA, Ross AE, Pienta KJ, Tran PT, Schaeffer EM. Oligometastatic prostate cancer: definitions, clinical outcomes, and treatment considerations. *Nat Rev Urol.* 2017;14:15-25.

7. Rowe SP, Macura KJ, Mena E, et al. PSMA-Based [(18)F]DCFPyL PET/CT Is Superior to Conventional Imaging for Lesion Detection in Patients with Metastatic Prostate Cancer. *Mol Imaging Biol.* 2016;18:411-419.

8. Perera M, Papa N, Christidis D, et al. Sensitivity, Specificity, and Predictors of Positive (68)Ga-Prostate-specific Membrane Antigen Positron Emission Tomography in Advanced Prostate Cancer: A Systematic Review and Meta-analysis. *Eur Urol.* 2016;70:926-937.

9. Rowe SP, Mana-Ay M, Javadi MS, et al. PSMA-Based Detection of Prostate Cancer Bone Lesions With (1)(8)F-DCFPyL PET/CT: A Sensitive Alternative to ((9)(9)m)Tc-MDP Bone Scan and Na(1)(8)F PET/CT? *Clin Genitourin Cancer.* 2016;14:e115-118.

10. Afshar-Oromieh A, Zechmann CM, Malcher A, et al. Comparison of PET imaging with a (68)Ga-labelled PSMA ligand and (18)F-choline-based PET/CT for the diagnosis of recurrent prostate cancer. *Eur J Nucl Med Mol Imaging.* 2014;41:11-20.

11. Morigi JJ, Stricker PD, van Leeuwen PJ, et al. Prospective Comparison of 18F-Fluoromethylcholine Versus 68Ga-PSMA PET/CT in Prostate Cancer Patients Who Have Rising PSA After Curative Treatment and Are Being Considered for Targeted Therapy. *J Nucl Med.* 2015;56:1185-1190.

12. Eiber M, Maurer T, Souvatzoglou M, et al. Evaluation of Hybrid (6)(8)Ga-PSMA Ligand PET/CT in 248 Patients with Biochemical Recurrence After Radical Prostatectomy. *J Nucl Med.* 2015;56:668-674.

13. Afshar-Oromieh A, Holland-Letz T, Giesel FL, et al. Diagnostic performance of (68)Ga-PSMA-11 (HBED-CC) PET/CT in patients with recurrent prostate cancer: evaluation in 1007 patients. *Eur J Nucl Med Mol Imaging.* 2017;44:1258-1268.

14. Rowe SP, Pienta KJ, Pomper MG, Gorin MA. Proposal for a Structured Reporting System for Prostate-Specific Membrane Antigen-Targeted PET Imaging: PSMA-RADS Version 1.0. *J Nucl Med.* 2018;59:479-485.

15. Rowe SP, Pienta KJ, Pomper MG, Gorin MA. PSMA-RADS Version 1.0: A Step Towards Standardizing the Interpretation and Reporting of PSMA-targeted PET Imaging Studies. *Eur Urol.* 2018;73:485-487.

16. Sheikhbahaei S, Afshar-Oromieh A, Eiber M, et al. Pearls and pitfalls in clinical interpretation of prostate-specific membrane antigen (PSMA)-targeted PET imaging. *Eur J Nucl Med Mol Imaging.* 2017;44:2117-2136.

17. Salas Fragomeni RA, Amir T, Sheikhbahaei S, et al. Imaging of Nonprostate Cancers Using PSMA-Targeted Radiotracers: Rationale, Current State of the Field, and a Call to Arms. *J Nucl Med.* 2018;59:871-877.

18. Ravert HT, Holt DP, Chen Y, et al. An improved synthesis of the radiolabeled prostate-specific membrane antigen inhibitor, [(18) F]DCFPyL. *J Labelled Comp Radiopharm.* 2016;59:439-450.

19. Rowe SP, Gorin MA, Hammers HJ, et al. Imaging of metastatic clear cell renal cell carcinoma with PSMA-targeted (1)(8)F-DCFPyL PET/CT. *Ann Nucl Med.* 2015;29:877-882.

20. Werner RA, Andree C, Javadi MS, et al. A Voice From the Past: Rediscovering the Virchow Node With Prostate-specific Membrane Antigen-targeted (18)F-DCFPyL Positron Emission Tomography Imaging. *Urology.* 2018;117:18-21.

21. Wahl RL, Jacene H, Kasamon Y, Lodge MA. From RECIST to PERCIST: Evolving Considerations for PET response criteria in solid tumors. *J Nucl Med.* 2009;50 Suppl 1:122S-150S.

22. Fanti S, Minozzi S, Morigi JJ, et al. Development of standardized image interpretation for 68Ga-PSMA PET/CT to detect prostate cancer recurrent lesions. *Eur J Nucl Med Mol Imaging.* 2017;44:1622-1635.

23. Eiber M, Herrmann K, Calais J, et al. Prostate Cancer Molecular Imaging Standardized Evaluation (PROMISE): Proposed miTNM Classification for the Interpretation of PSMA-Ligand PET/CT. *J Nucl Med.* 2018;59:469-478.

24. Orel SG, Kay N, Reynolds C, Sullivan DC. BI-RADS categorization as a predictor of malignancy. *Radiology.* 1999;211:845-850.

25. Weinreb JC, Barentsz JO, Choyke PL, et al. PI-RADS Prostate Imaging - Reporting and Data System: 2015, Version 2. *Eur Urol.* 2016;69:16-40.

26. Balleyguier C, Ayadi S, Van Nguyen K, Vanel D, Dromain C, Sigal R. BIRADS classification in mammography. *Eur J Radiol.* 2007;61:192-194.

27. Eisenhauer EA, Therasse P, Bogaerts J, et al. New response evaluation criteria in solid tumours: revised RECIST guideline (version 1.1). *Eur J Cancer.* 2009;45:228-247.

Tables and Table Legends

Table 1. Clinical and demographic data at the time of baseline ^{18}F-DCFPyL PET/CT scan from patients included in this study.

Patient Number	Age (y)	Serum Prostate-Specific Antigen (ng/ml)	Prior PCa Therapy	PCa Therapy After Baseline ^{18}F-DCFPyL PET/CT
1	66	4.6	Prostatectomy	Salvage Radiation, ADT
2	69	7.8	Prostatectomy	Salvage Radiation, SBRT, ADT
3	56	3.9	Neoadjuvant Taxotere, Neoadjuvant ADT, Prostatectomy	SBRT
4	66	6.48	Prostatectomy, Salvage Radiation, ADT, SBRT, Provenge, ^{177}Lu-PSMA	Taxotere
5	68	22.3	Prostatectomy, Salvage Radiation, Investigational DNA-Based Vaccine	ADT
6	63	12	Prostatectomy, ADT	ABRT, Provenge, Enzalutamide
7	66	0.4	Prostatectomy, Salvage Radiation, ADT	None
8	65	0.5	Taxotere, ADT, SBRT, Provenge	Provenge, SBRT, ^{177}Lu-PSMA
9	61	0.3	Prostatectomy	Salvage Radiation
10	65	37.8	None	EBRT, ADT
11	71	10.8	None	Prostatectomy
12	63	2.2	Prostatectomy, ADT	ADT
13	59	5.8	Prostatectomy, Salvage Radiation, ADT	SBRT
14	64	34.3	Prostatectomy, Salvage Radiation, ADT, Investigational DNA-Based Vaccine	ADT

15	53	23.3	None	Taxotere, ADT
16	64	5.6	Prostatectomy, Salvage Radiation, ADT, ^{177}Lu-PSMA, Provenge, Enzalutamide	Abiraterone
17	69	1.4	Prostatectomy, Salvage Radiation	ADT
18	50	0.7	Prostatectomy	Taxotere, ADT
19	64	70.4	None	Taxotere, ADT
20	54	21.4	None	Prostatectomy, Abiraterone, ADT
21	69	5.3	Prostatectomy, Salvage Radiation, ADT, ^{177}Lu-PSMA, SBRT	ADT, Carboplatin, Etoposide
22	63	9.7	None	ADT

*Abbreviations: ADT = androgen deprivation therapy; SBRT = stereotactic body radiation therapy; EBRT = external beam radiation therapy

Table 2. Characteristics of PSMA-RADS-3A and PSMA-RADS-3B lesions.

PSMA-RADS Score	Number of Lesions	Median SUV_{max} (Range)	Number of Lesions with Imaging Changes Suggesting Malignancy at Follow-Up (%)	Median SUV_{max} of Changed Lesions (Range)	Number of Unchanged Lesions on Follow-Up (%)	Median SUV_{max} of Changed Lesions (Range)
3A	32	1.62 (0.93 – 2.32)	24 (75%)	1.59 (1.05 – 2.32)	8 (25%)	1.62 (0.93 – 2.09)
3B	14	1.15 (0.85-1.89)	3 (21%)	1.35 (1.23 – 1.89)	11 (79%)	1.00 (0.85 – 1.54)
Total	46	1.44 (0.85-2.32)	27 (59%)	1.53 (1.05 – 2.32)	19 (41%)	1.30 (0.85 – 2.09)

Figure Legends

Figure 1. (A) Axial attenuation correction CT, (B) axial ^{18}F-DCFPyL PET, and (C) axial ^{18}F-DCFPyL PET/CT from a patient with a 3-mm short axis, pre-aortic, retroperitoneal lymph node with faint radiotracer uptake slightly higher than blood pool (red arrowheads). This was determined by central review to be a PSMA-RADS-3A lesion. (D) Follow-up axial attenuation correction CT, (E) axial ^{18}F-DCFPyL PET, and (F) axial ^{18}F-DCFPyL PET/CT six months later after multiple treatment modalities including androgen deprivation therapy. The node had definitively decreased in size and lacked any discernable uptake on the follow-up scan (red arrowheads), most compatible with PCa involvement.

Figure 2. (A) Axial attenuation correction CT, (B) axial ^{18}F-DCFPyL PET, and (C) axial ^{18}F-DCFPyL PET/CT from a patient with faint uptake in the inferior right scapula (red arrowheads). This was determined on central review to represent a PSMA-RADS-3B lesion without a visible anatomic correlate. (D) Follow-up axial attenuation correction CT, (E) axial ^{18}F-DCFPyL PET, and (F) axial ^{18}F-DCFPyL PET/CT 10 months later show markedly increased radiotracer uptake and new sclerosis in the inferior right scapula (red arrowheads), most consistent with a PCa bone metastasis. The patient had started on taxotere chemotherapy but had a rising prostate specific antigen level at the time of follow-up imaging, consistent with progressive systemic disease.

Figure 1.

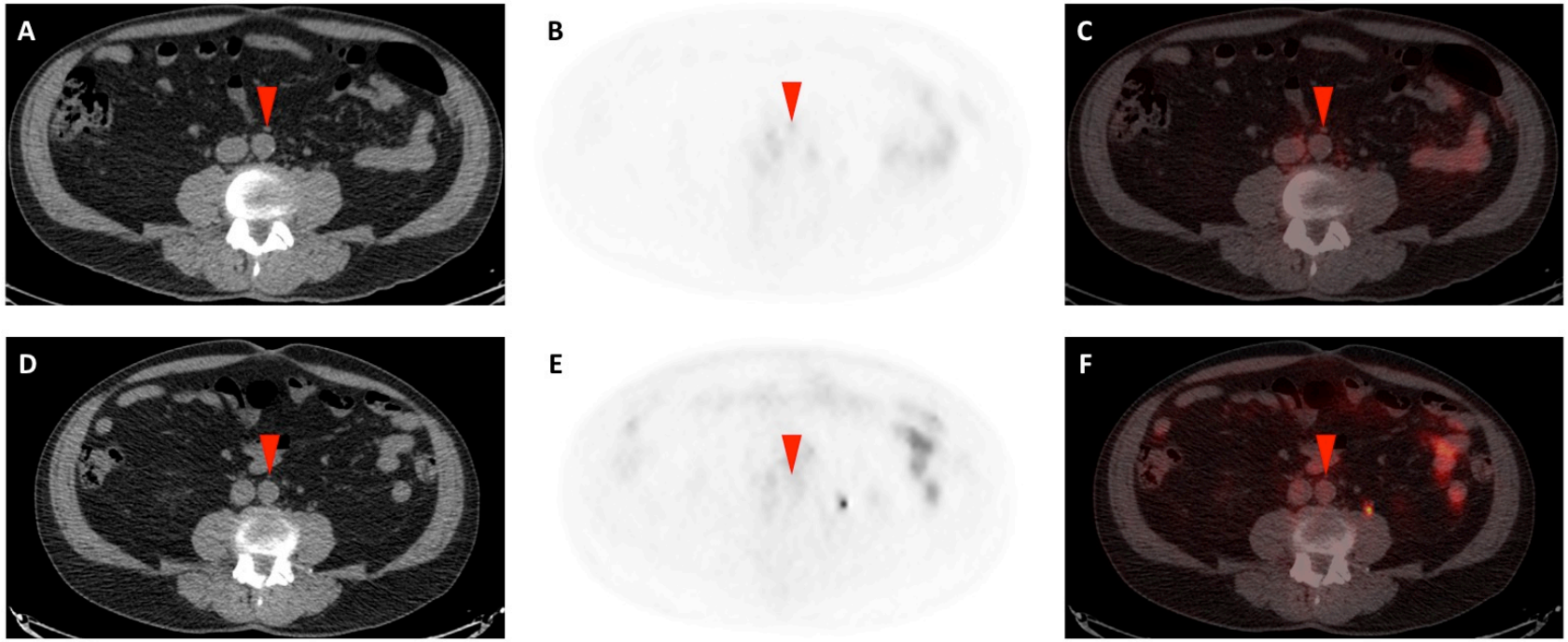

Figure 2.